

Cite this: DOI: 10.1039/c3cy00254c

CuAu/SiO₂ catalysts for the selective oxidation of propene to acrolein: the impact of catalyst preparation variables on material structure and catalytic performance†

Stéphanie Belin,^a Charlotte L. Bracey,^b Valérie Briois,^a Peter R. Ellis,^{*c} Graham J. Hutchings,^b Timothy I. Hyde^c and Gopinathan Sankar^{cd}

CuAu/SiO₂ catalysts are active and selective for the synthesis of acrolein from propene by selective oxidation using a mixture of H₂ and O₂ as oxidant. The catalyst synthesis method (impregnation or deposition) and the activation procedure (reduction, calcination or reduction followed by calcination and the choice of reducing agent) all affect the structure of the catalyst and therefore the performance in catalysis. For a material prepared by coimpregnation of H₂AuCl₄ and Cu(NO₃)₂, reduction with hydrogen leads to a catalyst with a significant level of CuAu alloy, whilst reduction with NaBH₄ solution leads to small particles but with negligible interaction between copper and gold. Subsequent high temperature calcination of these materials destroys any CuAu phase but retains a Cu–Au interaction as observed by Transmission Electron Microscopy. Preparation of the catalyst by a two-step deposition method gives smaller particles than coimpregnation when reduced by H₂ but a different alloy phase is observed by EXAFS. Calcination of this material gives a catalyst which combines high activity with excellent selectivity to acrolein. Characterisation of the materials using various techniques allows the nature of the active sites to be understood.

Received 15th April 2013,

Accepted 6th June 2013

DOI: 10.1039/c3cy00254c

www.rsc.org/catalysis

Introduction

Designing catalysts for selective oxidation reactions poses a significant challenge. With the notable exception of CO oxidation, the mechanism of the reaction and the structure of the catalysts needed to give good performance are not generally well understood. Yet the controlled introduction of oxygenated functionality into molecules is desirable for the sustainable production of a wide range of chemical products. To successfully synthesise catalysts for these reactions needs a good understanding of structure–function relationships; that is, how changes to the structure of the catalyst affect the activity, selectivity and stability of the catalyst in the reaction. In this

paper we address this topic for the selective oxidation of propene using bimetallic CuAu/SiO₂ catalysts.

CuAu catalysts have been found to be active for a number of oxidation reactions,¹ including the selective oxidation of CO,² propene,^{3–6} toluene⁴ and alcohols.^{7–9} These materials are complex, with many factors having an influence on the structure and catalytic performance of the final material. These include preparation method, which in turn determines the final oxidation states of copper and gold on the catalyst and whether they are present as a bimetallic phase or in a segregated form. The catalytic performance is further influenced by reaction conditions such as temperature, space velocity and the composition of the gas mixture – which contains both oxidising and reducing components.

Understanding the role of CuAu catalysts in propene oxidation presents a particular challenge since both metals are active catalysts in their own right. Copper catalysts on a range of supports have been used in the selective oxidation of propene. The major product from this oxidation pathway is typically acrolein. There is evidence that copper metal,¹⁰ Cu₂O¹¹ and CuO¹² all possess some activity in alkene selective oxidation. Cu₂O in particular is reported as being a highly selective phase in propene oxidation whilst CuO leads to combustion.¹¹ In addition, copper catalysts are used in the total oxidation of organic compounds – including propene¹³ – and

^a Synchrotron Soleil, L'Orme des Merisiers, Saint-Aubin, BP 48 91192 Gif-sur-Yvette CEDEX, France

^b Cardiff Catalysis Institute, School of Chemistry, Cardiff University, Park Place, Cardiff CF10 3AT, UK

^c Johnson Matthey Technology Centre, Blount's Court, Sonning Common, Reading RG4 9NH, UK. E-mail: ellispr@matthey.com

^d Department of Chemistry, University College London, 20 Gordon Street, London WC1H 0AJ, UK

† Electronic supplementary information (ESI) available. See DOI: 10.1039/c3cy00254c

the selective reduction of nitrogen oxides using propene as reducing agent.¹⁴ Gold catalysts, meanwhile have been shown to be active for the selective oxidation of propene to propene oxide.¹⁵ Here, a catalyst containing gold nanoparticles supported on reducible oxide supports such as TiO₂, titanosilicates or iron oxide is preferred as the interfacial site is thought to be important.¹⁶ In contrast to copper, gold catalysts for propene oxidation are typically used with hydrogen as a co-reductant, forming a hydroperoxy-type intermediate.

CuAu catalysts are known to be active for the selective oxidation of propene, and the structure of the catalyst and reaction conditions determine the spectrum of products and propene conversion observed. Sinfelt and Barnett⁴ used a coimpregnated CuAu/SiO₂ catalyst to oxidise propene to acrolein at temperatures of 265–305 °C with O₂ as oxidant. They found that reduction of the catalyst with hydrogen followed by high temperature calcination gave a material which could convert up to 40% of the propene present with acrolein selectivities of 50–70%. We also studied impregnated CuAu/SiO₂ catalysts³ and found that hydrogen co-feeding generally increased activity. The performance of reduced and reduced-calcined catalysts was compared; reduced catalysts contained a number of different active sites and gave a mixed selectivity profile, whilst reduced-calcined catalysts were generally more selective to acrolein. Llorca *et al.* have studied CuAu/TiO₂ catalysts prepared using coimpregnated precursors⁵ with N₂O as oxidant in their studies rather than O₂ or H₂/O₂. At 300 °C, a range of products were observed: propene oxide, propanal, acetone, acrolein and CO₂. The catalysts were shown by XRD and TEM to contain significant quantities of CuAu alloy phases. Catalysts which contained preformed thiol-stabilised CuAu nanoparticles⁶ were more active and gave up to 40% selectivity to propene oxide, although the other products were still observed. There is therefore a consensus that catalysts which contain CuAu alloys are not selective to a single product in propene oxidation. Au/CuO/Al₂O₃ catalysts have been found to be active for the total oxidation of propene to carbon dioxide and water¹⁷ at around 200 °C using an excess of oxygen (propene : oxygen = 1 : 9). The catalysts were reduced at 300 °C prior to catalysis, although alloying of gold and copper was not observed.

In this paper we explore the impact of catalyst synthesis method – either by impregnation using copper nitrate and tetrachloroauric acid, or by a two-step deposition method – and the effect of different activating treatments – reduction with hydrogen or NaBH₄ solution followed optionally by a high temperature calcination – on the structure of the catalyst produced and the performance in the selective oxidation of propene using a mixture of H₂ and O₂ as oxidant.

Experimental

Catalyst preparation

Materials. Copper nitrate hemipentahydrate, sodium borohydride, basic copper carbonate, sodium hydroxide, ammonium carbonate (Alfa Aesar), ammonium hydroxide solution (35%, Fisher) tetrachloroauric acid (41.63% Au, Johnson Matthey) and silica (Grace P432, reference SP550-SP10022, BET surface area 340 m² g⁻¹) were all used as received.

Impregnation synthesis. The pore volume of the silica was measured by adding water until the incipient wetness point was reached, and following the change in mass during the addition. A solution of copper nitrate hemipentahydrate (0.89 g, 38 mmol) and tetrachloroauric acid (1.83 g solution, 38 mmol) was prepared using the appropriate volume of water to fill the pores of the support and to give the desired concentration and ratio of metals in the final product. The impregnated material was dried at 105 °C for three hours.

Deposition synthesis. In this method, the copper and gold are added sequentially, the copper being added first. A solution of basic copper carbonate (0.76 g, 3.4 mmol salt, 6.9 mmol Cu) and ammonium carbonate (7.5 g, 85 mmol) was prepared in a mixture of ammonium hydroxide solution (85 ml) and water (75 ml). To this was added the silica support (36 g), and the suspension heated to boiling. Ammonia was removed by distillation causing the copper to deposit onto the support. The product of the reaction was collected by filtration, washed with water and dried at 105 °C for three hours. The dried Cu/SiO₂ (10 g) was re-suspended in water (400 ml) at 65 °C and gold was added by deposition precipitation using sodium hydroxide (0.1 M solution) as base and tetrachloroauric acid (0.89 g solution, 1.9 mmol) as gold precursor. The pH of the reaction was maintained around nine by appropriate addition rates of gold solution and base. The reaction product was isolated by filtration, washed with water and then dried at 105 °C for three hours.

Hydrogen reduction. Materials were reduced in 5% H₂/N₂ in a tube furnace. The temperature was increased to 40 °C at 2 °C min⁻¹ and held for 30 minutes to purge the tube. It was then further increased to 315 °C at 10 °C min⁻¹, holding at 315 °C for two hours then cooling to room temperature.

Sodium borohydride reduction. The dried precursor prepared by co-impregnation was impregnated for a second time with an aqueous solution of sodium borohydride. The reaction between the catalyst precursor and the sodium borohydride solution was strongly exothermic. The material was aged for one hour before being washed with water, filtered and dried at 105 °C for three hours.

Direct calcination. The impregnated catalyst was calcined directly without reduction. This was performed in a static air furnace by heating to 400 °C at 10 °C min⁻¹, holding for two hours and cooling to room temperature.

High temperature calcination. Selected reduced catalysts were subsequently calcined at high temperature. The calcination was performed in a static air furnace. The temperature was increased to 675 °C at 10 °C min⁻¹, holding at 675 °C for sixteen hours then cooling to room temperature.

Characterisation

The metal contents of the catalysts were determined by Inductively-coupled plasma electronic spectroscopy (ICP-ES) following digestion in *aqua regia*. The samples were analysed using a Perkin Elmer Optima instrument. XRD patterns were recorded on a Bruker D8 instrument between 10 and 130° 2 θ using Ni filtered Cu radiation. Crystallite sizes and lattice parameters were determined by Rietveld refinement using Bruker Topas V4 analysis software. Lattice parameter data was taken from the

ICDD Database, PDF-4 release 2012. The lattice parameters for copper (PDF 00-004-0836) and gold (00-004-0784) were 3.615 Å and 4.079 Å respectively. The lattice parameters for the monoclinic copper oxide (tenorite, PDF 00-048-1548) were $a = 4.684$ Å, $b = 3.425$ Å, $c = 5.129$ Å and $\beta = 99.47^\circ$. BET analyses were performed using a five-point method on a Quantachrome Autosorb instrument. TEM images were acquired using a Tecnai-F20 instrument. Powder samples were set in resin and sectioned for analysis, or the powder was dusted onto a holey carbon grid. Nickel TEM grids were used to avoid interference with the copper in the samples. Particle size was determined by an image contrast method. Diffuse Reflectance Visible Spectroscopy was performed on solid samples using an Agilent Cary Series Spectrometer with a Praying Mantis attachment. Samples were diluted with barium sulphate to increase the signal to noise ratio. The temperature-programmed reduction study in Fig. S7 (ESI[†]) was performed using a 5% Cu/SiO₂ catalyst containing copper(II) oxide. The catalyst was prepared by incipient wetness impregnation using copper nitrate and was calcined in air at 400 °C prior to the experiment. The TPR spectrum was obtained using an Altamira AMI-200 catalyst characterisation unit. The gas used was 30 ml min⁻¹ of 10% H₂/Ar and the heating rate was 10 °C min⁻¹.

X-Ray Absorption Spectroscopy was performed on the SAMBA beamline at Synchrotron Soleil, Paris, France. Data were collected at both the Cu K (8900–13 400 eV) and Au L3 (11 165–13 400 eV) edges in QuickEXAFS mode.¹⁸ Each scan lasted for 1 s. Typically around 200 spectra were combined to give good quality data for analysis. Spectra were referenced to Cu foil or Au foil. The data were analysed using the Athena¹⁹ software for data handling and XANES fitting. XANES spectra were fitted from –50 eV to +100 eV relative to the edge energy using normalised data. The fit quality values were used to rank the fits generated from different combinations of reference materials. Copper(II) oxide, copper(I) oxide, copper(II) nitrate hemipentahydrate and copper foil were used as standards at the copper edge, whilst sodium gold(III) chloride, sodium gold(I) thiosulphate and gold foil were the standards used at the gold edge. All of these standards were used in XANES fitting, although some were found not to be relevant. EXAFS data analysis was performed using Artemis¹⁹ in multi-edge mode fitting both Cu K and Au L3 edge data in the k -range from 2.5 to 12.

Catalyst testing

Propene oxidation was performed using a flow microreactor and the products were analysed using on-line gas chromatography.

The catalyst (0.2 g) was heated in a flow of reactant gases with a total space velocity of 22 500 h⁻¹. The gas mixture used was 1 : 1 : 1 : 7 H₂ : O₂ : C₃H₆ : He.²⁰ The high space velocity used makes the propene conversion values reported low. Reactions were started at 200 °C and increased in steps of 20 °C to a final temperature of 300 °C or 320 °C before being cooled back to 200 °C in 20 °C steps. The reaction was dwelled at each temperature for thirty minutes to allow steady-state data to be recorded. The hysteresis in reaction performance observed with temperature allowed changes in the catalyst during use to be assessed. Changes in activity and selectivity can be ascribed to different effects (sintering, poisoning, dealloying *etc.*) and so this is a sensitive probe to the structure of the catalyst.

Results

A series of seven catalysts were synthesised as described above. Their characterisation data are presented in Tables 1–5 and Fig. 1–6. Their catalytic performance is summarised in Table 6. Further details on the catalytic performance and XAS data analysis is available in the ESI.[†]

Impregnated catalyst, calcined only

Calcination of the precursor leads to a material with very little interaction between copper and gold. The copper is present as copper(II) oxide particles on the silica support, whilst the gold is present in large (micron-sized) clusters which are only weakly bound to the surface (Fig. 5). XAS analysis confirms the presence of gold metal and copper(II) species (Fig. 2–4) with values close to bulk materials (Table 4). The catalyst is poorly active and produces a mixture of acrolein, carbon dioxide and propene oxide (Table 6).

Impregnated catalyst, hydrogen reduction

Reducing the impregnated catalyst precursor with H₂ (315 °C, 2 h) gives a material with a stronger interaction between copper and gold, as indicated by the shift from 600 nm to 620 nm in the plasmon band in DR-visible spectroscopy (Fig. 6) compared with that of the calcined material. It is also accompanied by some quenching of the peak. XRD (Fig. 1) also indicates that CuAu species are present, but they are poorly defined and more than one environment may exist. EXAFS (Fig. 4 and Table 4), on the other hand, identifies the presence of copper–copper interactions as well as those of copper–oxygen, copper–gold and gold–gold. TEM (Fig. 5) detected large particles in the sample which contained both copper and gold. These will also be

Table 1 Summary of the catalysts synthesised and the copper and gold species present

Preparation method	Pretreatment	Phases observed					Particle size range
		Cu(II) oxide	Cu(I) oxide	Cu metal	Au metal	CuAu alloy	
Impregnation	Calcination	•			•		Large
	Reduction in H ₂	•		•	•	•	Large
	Reduction in H ₂ and calcinations	•			•		Large
	NaBH ₄ reduction	•			•		Large
	NaBH ₄ reduction and calcination	•			•		Large
Deposition	Reduction in H ₂	•			•	•	Small
	Reduction in H ₂ and calcination	•			•		Small

Table 2 ICP analysis, XRD average crystallite size and TEM determined particle size

Preparation method	Pretreatment	ICP data			XRD average crystallite size/nm (phase)	TEM particle size/nm (particles counted)
		Cu/wt%	Au/wt%	Cu/Au molar ratio		
Impregnation	Calcination	1.1	4.8 ^a	0.71	54 (Au)	^b
	Reduction in H ₂	1.35	3.28	1.28	14 (CuAu(1))	^b
					9 (CuAu(2))	
	Reduction in H ₂ and calcination	1.22	3.98	0.95	54 (Au)	7 (184)
	NaBH ₄ reduction	0.63	2.98	0.66	5 (Au)	24 (187)
NaBH ₄ reduction and calcination	0.66	3.39	0.60	11 (Au)	24 (35)	
Deposition	Reduction in H ₂	1.23	3.77	1.01	<2 (CuAu)	8 (191)
	Reduction in H ₂ and calcination	1.01	3.97	0.79	15 (Au)	6 (39)
					69 (CuO)	

^a Heterogeneity observed in these samples, the ICP value presented is an average of a number of replicates. ^b Not determined.

Table 3 XRD characterisation of catalysts

Preparation method	Pretreatment	Phases observed – crystallite size/nm (lattice parameter/Å)		
		Cu(II) oxide ^c	Au metal	CuAu alloy
CuAu/SiO ₂ catalysts Impregnation	Calcination		55 (4.07935(7))	
	Reduction in H ₂			14 (4.0460)
	Reduction in H ₂ and calcination	20 (<i>a</i> = 4.674(5) <i>b</i> = 3.427(3) <i>c</i> = 5.139(6) <i>β</i> = 99.54(7)°)	54 (4.07954(4))	9 (4.0069) ^b
Deposition	NaBH ₄ reduction		5 (4.0752)	
	NaBH ₄ reduction and calcination	^a	11 (4.0791)	
	Reduction in H ₂		<2 (4.0792)	
	Reduction in H ₂ and calcination	50 (<i>a</i> = 4.689(2) <i>b</i> = 3.427(3) <i>c</i> = 5.139(6) <i>β</i> = 99.54(7)°)	16 (4.0794(1))	
Cu/SiO ₂ catalyst Impregnation	Calcination	19 (<i>a</i> = 4.689(1) <i>b</i> = 3.431(1) <i>c</i> = 5.134(1) <i>β</i> = 99.46(1)°)		
Au/SiO ₂ catalyst Impregnation	Calcination		39 (4.0815)	
Literature values		<i>a</i> = 4.684 <i>b</i> = 3.425 <i>c</i> = 5.129 <i>β</i> = 99.47°	4.079	

^a Observed at low levels, no reliable crystallite size or lattice parameter data could be obtained. ^b Two distinct phases observed. ^c Tenorite has a monoclinic structure and hence is described by three lattice parameters and one angle (*β*). In this case $\alpha = \gamma = 90^\circ$.

detected by XRD and EXAFS but, at particle sizes of 100 nm and above, they are unlikely to impact significantly on catalysis. TEM also observes smaller particles on the catalyst (Fig. 5) but these are poorly defined and it is difficult to completely understand their nature.

The EXAFS results reported here are similar to those of Meitzner *et al.*²¹ Both studies observe Cu–Au and Cu–Cu interactions. The main difference is that in our sample we also observe Cu–O interactions. This may result from either the storage of the sample in air or the more rapid passivation on

removal from the tube furnace in our study. Meitzner *et al.* also report the ratio of Cu–Cu and Cu–Au coordination at the Cu edge as 2.7. In our study we find this ratio to be only 0.45. If the Cu–O interactions are considered to come from the oxidation of Cu–Cu interactions, then this increases to 1.9 (assuming that one Cu–Cu interaction yields two Cu–O interactions). At the gold edge, the reported ratio of Au–Cu to Au–Au is 0.41, compared with 0.28 in this study. Their Cu–Au bond length (2.68 ± 0.02 Å) is very close to the one reported in this work, 2.71 ± 0.02 Å.

Table 4 (A) Cu K edge EXAFS fit parameters. R = bond distance (\AA), N = coordination number, σ^2 = Debye–Waller factor. The measured fit index values were from 0.01 to 0.06. (B) Au L3 edge EXAFS fit parameters. R = bond distance (\AA), N = coordination number, σ^2 = Debye–Waller factor. The measured fit index values were 0.005 to 0.06

(A)		Cu–O			Cu–Cu			Cu–Au		
Preparation method	Pretreatment	$R/\text{\AA}$	N	$\sigma^2/\text{\AA}^2$	$R/\text{\AA}$	N	$\sigma^2/\text{\AA}^2$	$R/\text{\AA}$	N	$\sigma^2/\text{\AA}^2$
Impregnation	Calcination	1.95	4.3	0.008	—	—	—	—	—	—
	Reduction in H_2	1.92	2.2	0.008	2.55	1.4	0.006	2.75	3.1	0.014
	Reduction in H_2 and calcination	1.97	3.1	0.005	—	—	—	—	—	—
	NaBH_4 reduction	1.97	4.3	0.008	—	—	—	—	—	—
	NaBH_4 reduction and calcination	1.95	3.3	0.006	—	—	—	—	—	—
Deposition	Reduction in H_2	1.93	2.5	0.006	—	—	—	2.68	0.3	0.001
	Reduction in H_2 and calcination	1.96	3.1	0.006	—	—	—	—	—	—

(B)		Au–Cu			Au–Au		
Preparation method	Pretreatment	$R/\text{\AA}$	N	$\sigma^2/\text{\AA}^2$	$R/\text{\AA}$	N	$\sigma^2/\text{\AA}^2$
Impregnation	Calcination	—	—	—	2.88	7.8	0.008
	Reduction in H_2	2.75	2.0	0.014	2.86	7.2	0.008
	Reduction in H_2 and calcination	—	—	—	2.88	11.0	0.008
	NaBH_4 reduction	—	—	—	2.87	9.6	0.009
	NaBH_4 reduction and calcination	—	—	—	2.87	9.6	0.009
Deposition	Reduction in H_2	2.68	0.3	0.001	2.84	6.7	0.009
	Reduction in H_2 and calcination	—	—	—	2.88	10.3	0.008

Table 5 (A) Best fits of XANES data from Cu K edge spectra. The standards used in fitting were copper foil for Cu(0), Cu_2O for Cu(I) and for Cu(II) both CuO (A) and $\text{Cu}(\text{NO}_3)_2 \cdot 2.5\text{H}_2\text{O}$ (B) were applied. '—' means not included in fit. Fit quality values are reported in Table S2 (ESI). (B) Best fits of XANES data from Au L3 edge spectra. The standards used in fitting were gold foil for Au(0), $\text{Na}_3\text{Au}(\text{S}_2\text{O}_3)_2$ for Au(I) and NaAuCl_4 for Au(III). '—' means not included in fit. Fit quality values are reported in Table S3 (ESI)

(A)		Fit/%			
Preparation method	Pretreatment	Cu(II) (A)	Cu(II) (B)	Cu(I)	Cu(0)
Impregnation	Calcination	51.9	48.1	—	—
	Reduction in H_2	36.1	53.2	8.5	32.2
	Reduction in H_2 and calcination	61.6	38.4	—	—
	NaBH_4 reduction	50.8	49.2	—	—
	NaBH_4 reduction and calcination	54.6	45.4	—	—
Deposition	Reduction in H_2	41.7	22.5	17.1	18.7
	Reduction in H_2 and calcination	62.3	37.7	—	—

(B)		Fit/%		
Preparation method	Pretreatment	Au(0)	Au(I)	Au(III)
Impregnation	Calcination	100	—	—
	Reduction in H_2	60.4	39.6	—
	Reduction in H_2 and calcination	100	—	—
	NaBH_4 reduction	100	—	—
	NaBH_4 reduction and calcination	100	—	—
Deposition	Reduction in H_2	74.4	25.6	—
	Reduction in H_2 and calcination	100	—	—

This catalyst also demonstrates poor catalytic activity, although it is approximately twice as active as the calcined impregnated catalyst. The catalyst produces a mixture of products which suggests that multiple active sites are present (Table 6).

Impregnated catalyst, hydrogen reduced and calcined

This is the material described by Sinfelt and Barnett⁴ and it performs much better than the reduced or calcined impregnated materials. Although it is less active than the reduced

impregnated catalyst, the selectivity to acrolein is significantly higher, and other oxygenated products are no longer produced (Table 6). XRD (Fig. 1) and EXAFS (Fig. 4 and Table 4) show that there are no crystalline CuAu alloy species in this catalyst, rather the copper is present as copper(II) oxide and the gold as gold metal. There is some evidence from TEM (Fig. 5) that the copper and gold species are in close proximity to each other, unlike in the calcined material where they are physically remote.

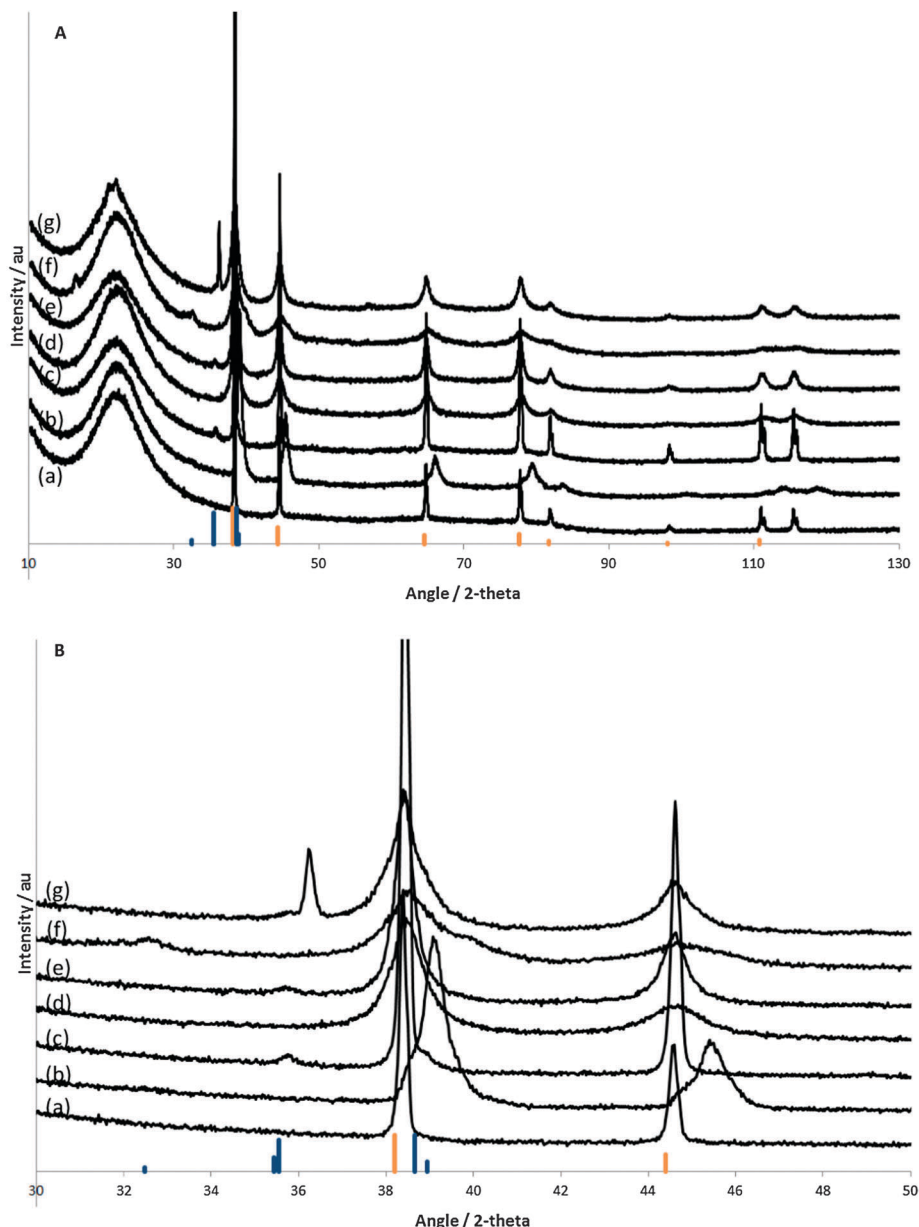


Fig. 1 (A) XRD patterns of CuAu/SiO₂ prepared by coimpregnation and (a) calcined; (b) reduced in H₂; (c) reduced in H₂ and calcined; (d) reduced using NaBH₄ solution; (e) reduced using NaBH₄ solution and calcined; CuAu/SiO₂ prepared by deposition and (f) reduced in H₂; (g) reduced in H₂ and calcined; the gold bars refer to the expected positions of reflections due to Au metal, and the blue bars to the expected positions of peaks due to CuO (tenorite). (B) Expansion of XRD patterns of CuAu/SiO₂ prepared by coimpregnation and (a) calcined; (b) reduced in H₂; (c) reduced in H₂ and calcined; (d) reduced using NaBH₄ solution; (e) reduced using NaBH₄ solution and calcined; CuAu/SiO₂ prepared by deposition and (f) reduced in H₂; (g) reduced in H₂ and calcined; the gold bars refer to the expected positions of reflections due to Au metal, and the blue bars to the expected positions of peaks due to CuO (tenorite).

Impregnated catalyst, sodium borohydride reduction

Reduction of the catalyst with NaBH₄ was highly exothermic. It is also expected to be a more rapid reduction than using hydrogen. TEM shows that the particle size is much smaller than for the hydrogen-reduced material (Fig. 5), but nevertheless the catalyst activity is similar. The NaBH₄ reduction does not lead to the formation of an appreciable amount of CuAu alloy phase. EDX suggests that the particles contain both copper and gold, but are very gold rich. However, neither EXAFS

(Fig. 4 and Table 4) nor XRD (Fig. 1) detect a CuAu phase, instead showing that gold is present as metallic nanoparticles and copper as copper(II) oxide. Given that the structure of this material is quite different to that reduced using hydrogen, it is not surprising that the catalytic performance is also different. The only products observed are acrolein and carbon dioxide, and the acrolein selectivity is good at 84% (Table 6). The product distribution observed is very similar to that of the reduced and calcined material described above, which is a consequence of the catalysts containing the same metal species.

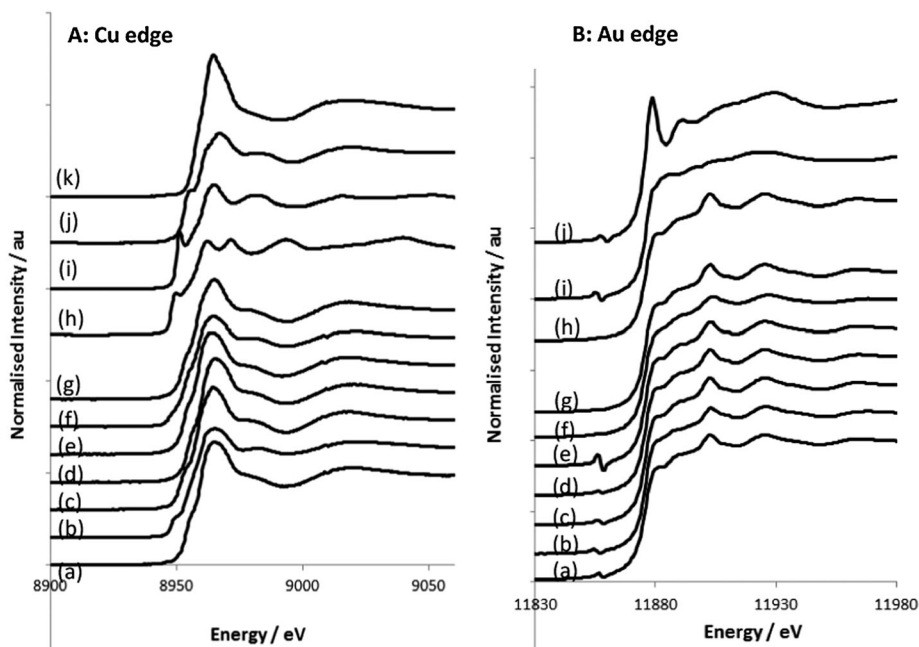


Fig. 2 (A) Cu-K edge XANES data for CuAu/SiO₂ prepared by coimpregnation and (a) calcined; (b) reduced in H₂; (c) reduced in H₂ and calcined; (d) reduced using NaBH₄ solution; (e) reduced using NaBH₄ solution and calcined; CuAu/SiO₂ prepared by deposition and (f) reduced in H₂; (g) reduced in H₂ and calcined; (h) Cu foil; (i) Cu₂O; (j) CuO and (k) Cu(NO₃)₂·2.5H₂O. (B) Au-L3 edge XANES data for CuAu/SiO₂ prepared by coimpregnation and (a) calcined; (b) reduced in H₂; (c) reduced in H₂ and calcined; (d) reduced using NaBH₄ solution; (e) reduced using NaBH₄ solution and calcined; CuAu/SiO₂ prepared by deposition and (f) reduced in H₂; (g) reduced in H₂ and calcined; (h) Au foil; (i) Na₃Au(S₂O₃)₂ and (j) NaAuCl₄.

Sodium borohydride reduction has previously been applied to CuAu catalyst preparation.⁷ In this case the metals were added sequentially with NaBH₄ treatment after each addition, followed by calcination at 250 °C. As with our experience, no CuAu alloy phase was observed on the catalyst.

Impregnated catalyst, sodium borohydride reduced and calcined

Calcination of the NaBH₄-reduced material sinters the gold and copper oxide particles, as shown by both XRD (Fig. 1) and EXAFS (Fig. 4 and Table 4). This makes the catalyst less active; indeed, it is the least active of all the catalysts reported in this paper, although the selectivity to acrolein is high (Table 6). TEM shows that the small particles on the catalyst have an interesting structure (Fig. 5) where the gold and copper oxide particles are next to each other or even in contact on the support, suggesting that they have been dealloyed and sintered. This is not observed in the NaBH₄-reduced material, so is likely to have occurred during the calcination step.

This catalyst is the least active of all the materials studied, although in common with other reduced-calcined catalysts it shows good selectivity to acrolein, with no oxygenates being produced (Table 6).

Deposition catalyst, hydrogen reduction

The first important difference between the deposition and impregnation routes is in dispersion. Here there are many fewer large particles, so the peaks in the XRD spectrum (Fig. 1) are broad and weak, in contrast to the impregnated catalyst.

TEM (Fig. 5) does not show the large copper-gold particles found in the impregnated sample. DR-visible spectroscopy (Fig. 6) suggests that a CuAu phase is present in at least part of the sample, as the plasmon peak is shifted from the value expected for monometallic gold, and indeed EXAFS (Fig. 4 and Table 4) also finds a small amount of gold alloy (Cu-Au coordination number 0.3). However, most of the gold is present as gold metal and the copper as copper(II) species.

This material performs well as a catalyst, with a much higher activity than any of the impregnated catalysts (Table 6). The selectivity to acrolein is also high, indicating that only one major type of active site is present in the material.

Deposition catalyst, hydrogen reduced and calcined

High temperature calcination of the hydrogen-reduced material leads to the destruction of all CuAu alloy species on the catalyst, as shown by DR-visible spectroscopy (Fig. 6), XRD (Fig. 1) and XAS (Fig. 2–4 and Table 4). The gold and copper oxide particles are still quite small (5–10 nm by TEM (Fig. 5)) despite the high temperature treatment. Unlike the impregnated catalysts, high temperature calcination of the reduced catalyst increases its activity markedly; this is by far the most active of the catalysts reported in this paper. Selectivity to acrolein is also good. The performance of this material compared with the impregnated catalyst hydrogen reduced and calcined is presented in Fig. 7. Here, at 320 °C the propene conversion is just over 10% and the selectivity to acrolein 89% with small amounts of ethanal and carbon dioxide observed as by-products.

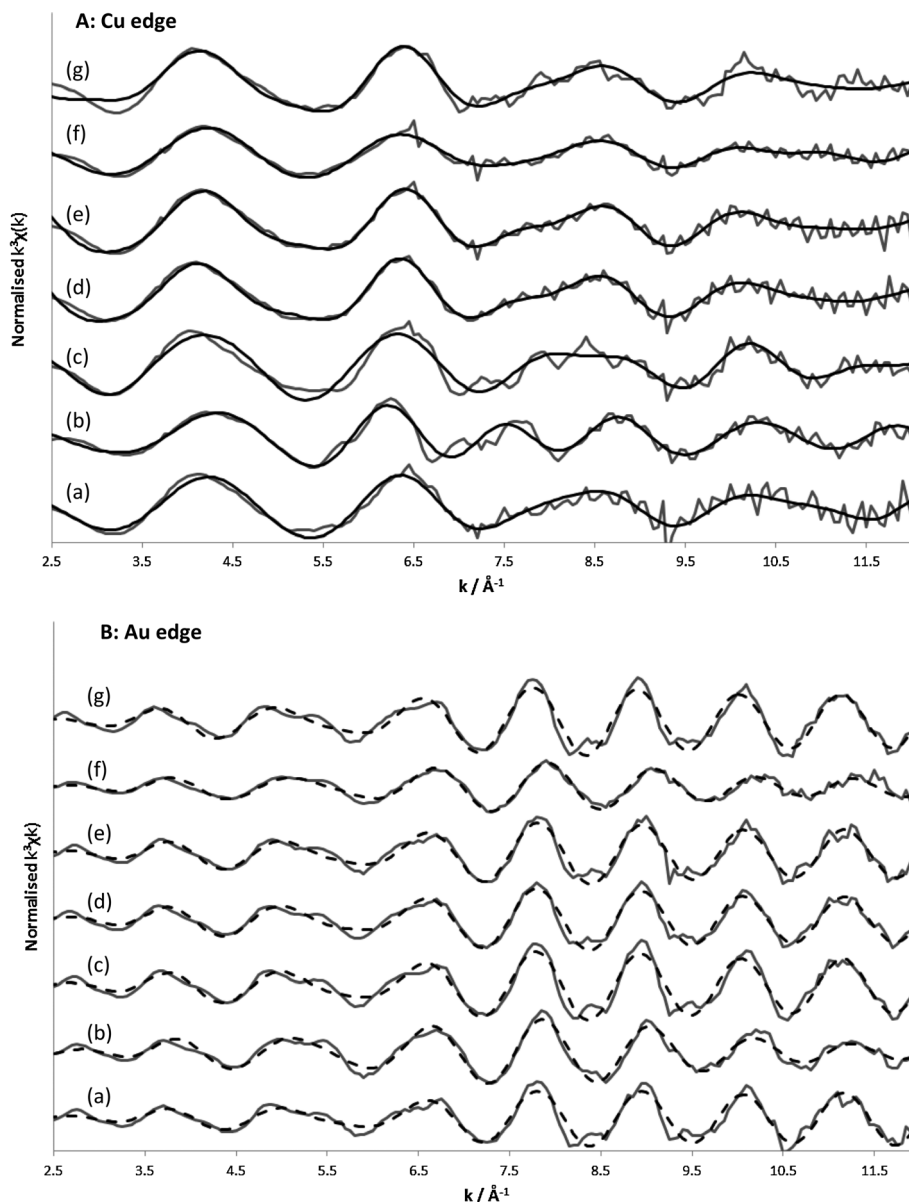


Fig. 3 (A) Cu-K edge EXAFS data (as k^3) for CuAu/SiO₂ prepared by coimpregnation and (a) calcined; (b) reduced in H₂; (c) reduced in H₂ and calcined; (d) reduced using NaBH₄ solution; (e) reduced using NaBH₄ solution and calcined; CuAu/SiO₂ prepared by deposition and (f) reduced in H₂; (g) reduced in H₂ and calcined. (B) Au-L3 edge EXAFS data (as k^3) for CuAu/SiO₂ prepared by coimpregnation and (a) calcined; (b) reduced in H₂; (c) reduced in H₂ and calcined; (d) reduced using NaBH₄ solution; (e) reduced using NaBH₄ solution and calcined; CuAu/SiO₂ prepared by deposition and (f) reduced in H₂; (g) reduced in H₂ and calcined.

Discussion

XAS data analysis

XAS analysis is an excellent technique for understanding the structure of bimetallic catalysts, which tend to be poorly crystalline and contain many metal species: oxidised and reduced, bimetallic and monometallic. We have analysed both the XANES and EXAFS parts of the data to help understand the structure of the catalysts tested.

Initial attempts to fit the Cu edge XANES data were made using three standards: CuO, Cu₂O and Cu metal foil. However, for most of the catalysts this did not give a satisfactory fit (see ESI†). To improve the fit required the addition of a new

standard, copper(II) nitrate hemipentahydrate. The materials which had been calcined or reduced and calcined could be fitted well with a mixture of copper(II) oxide and copper(II) nitrate hemipentahydrate with no contribution from either copper(I) oxide or copper metal foil (Table 5). The materials do not of course contain copper nitrate as they have all been thermally treated at temperatures where copper nitrate would be decomposed, or reacted with sodium borohydride which would have the same effect. Copper(II) oxide and copper(II) nitrate have different co-ordination environments – copper(II) oxide has four nearest neighbour oxygen atoms at 1.941 Å distance in an approximately square planar arrangement²² whilst copper(II) nitrate contains a distorted octahedron of

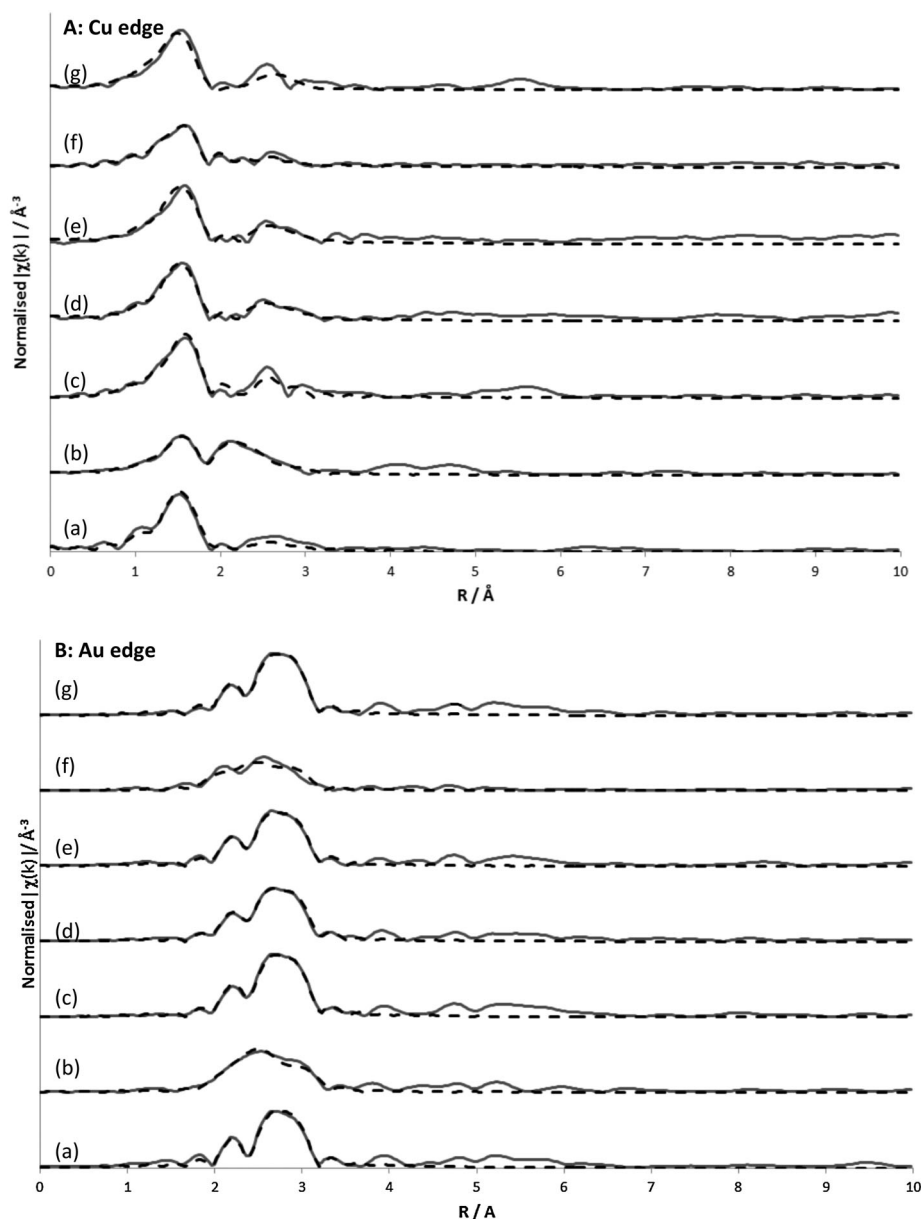


Fig. 4 (A) Fourier-transform Au-L3 edge EXAFS data for CuAu/SiO₂ prepared by coimpregnation and (a) calcined; (b) reduced in H₂; (c) reduced in H₂ and calcined; (d) reduced using NaBH₄ solution; (e) reduced using NaBH₄ solution and calcined; CuAu/SiO₂ prepared by deposition and (f) reduced in H₂; (g) reduced in H₂ and calcined. (B) Fourier-transform Au-L3 edge EXAFS data for CuAu/SiO₂ prepared by coimpregnation and (a) calcined; (b) reduced in H₂; (c) reduced in H₂ and calcined; (d) reduced using NaBH₄ solution; (e) reduced using NaBH₄ solution and calcined; CuAu/SiO₂ prepared by deposition and (f) reduced in H₂; (g) reduced in H₂ and calcined. Data is not phase corrected.

Cu–O distances due to the Jahn–Teller effect: four shorter bonds of 1.959 Å and two longer bonds at 1.99 Å. A seventh Cu–O interaction with a neighbouring unit cell at 2.39 Å completes the coordination environment in the solid state.²³ One interpretation of the Cu edge XANES data is the characterisation of ‘bulk-like’ copper oxide, represented by CuO, and ‘well-dispersed’ CuO species, represented by Cu(NO₃)₂·2.5H₂O. The ratio of these two species is similar across all the calcined and reduced-calcined samples, with the CuO contribution varying from 50% to 63%. An alternative explanation for the Cu edge XANES data is that the spectrum shows a single copper

environment which is intermediate between CuO (square planar) and Cu(NO₃)₂·2.5H₂O, which is a distorted octahedron. This is supported by the absence of crystalline CuO from the XRD of many of the samples. It is interesting in light of the reported good selectivity of Cu₂O in propene oxidation¹¹ that no evidence for this oxidation state was found.

Fitting the two hydrogen-reduced samples was hampered by the lack of a suitable standard material for CuAu alloy phases. The impregnated catalyst reduced with hydrogen was fitted with a combination of four standards whilst the deposition catalyst reduced with hydrogen was fitted with three (Table 5).

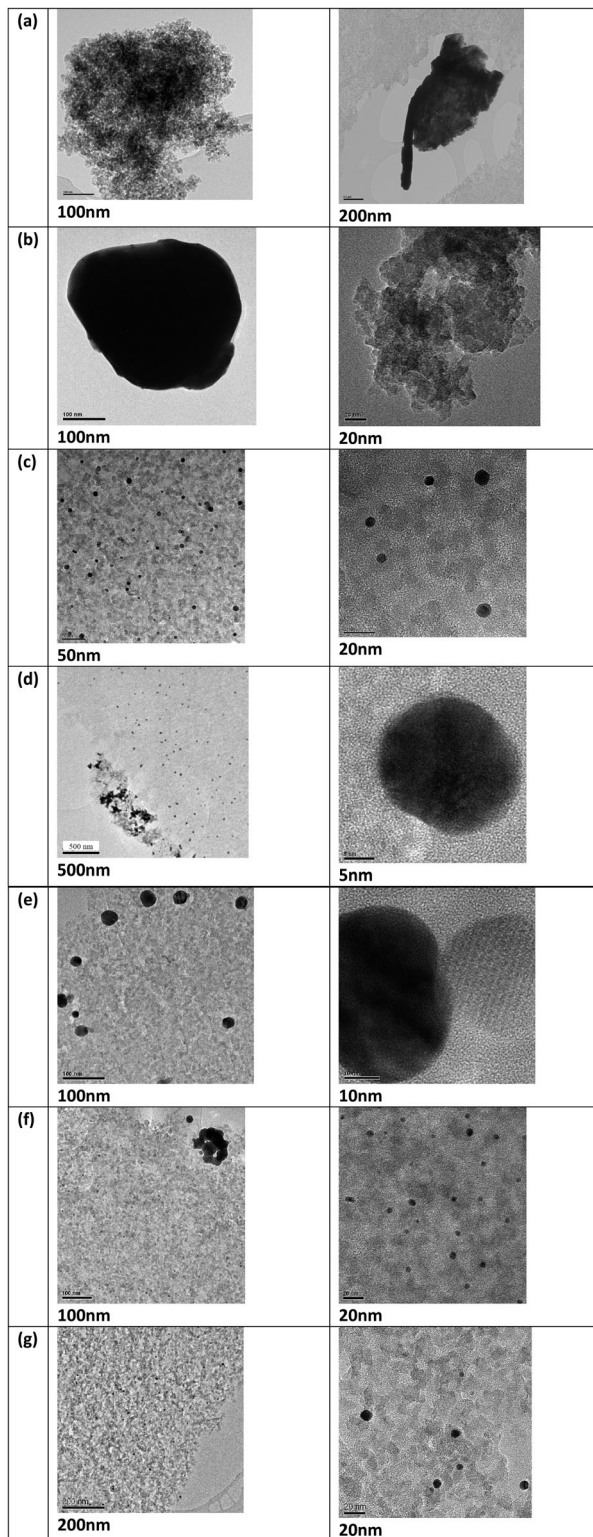


Fig. 5 TEM data for CuAu/SiO₂ prepared by coimpregnation and (a) calcined; (b) reduced in H₂; (c) reduced in H₂ and calcined; (d) reduced using NaBH₄ solution; (e) reduced using NaBH₄ solution and calcined; CuAu/SiO₂ prepared by deposition and (f) reduced in H₂; (g) reduced in H₂ and calcined.

However, these fits may not be meaningful in the absence of a copper-gold reference material.

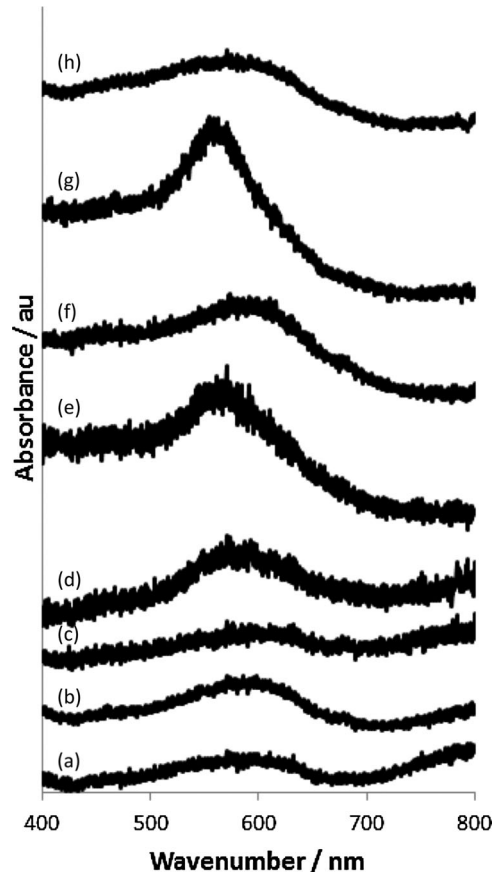


Fig. 6 Diffuse Reflectance Visible Spectra of CuAu/SiO₂ prepared by coimpregnation and (a) calcined; (b) reduced in H₂; (c) reduced in H₂ and calcined; (d) reduced using NaBH₄ solution; (e) reduced using NaBH₄ solution and calcined; CuAu/SiO₂ prepared by deposition and (f) reduced in H₂; (g) reduced in H₂ and calcined; and (h) a 5% Au/SiO₂ reference material prepared by HAuCl₄ impregnation.

The Au L3 edge XANES data, meanwhile, was initially fitted using three standards, one for each of the commonly-observed gold oxidation states. Gold metal foil was used to represent Au(0), Na₃Au(S₂O₃)₂ for Au(I) and NaAuCl₄ for Au(III). Whilst all the calcined and reduced-calcined materials could be fitted with a combination of the three standards, fitting using gold metal only is considered the best solution as the quality of the fits were similar in both cases (see ESI†). The two hydrogen-reduced samples were again different and were best fitted using a combination of gold metal foil and sodium gold thiosulphate.²⁴ Again this does not suggest the presence of sulphur in the materials, but is probably a mimic for the unreferenced CuAu phase. Fitting using a Au(I) standard may also show that the gold is slightly electron deficient in these materials, with electron density being transferred to copper.

Consideration of the EXAFS data confirms the XANES results above. All the calcined and reduced-calcined catalysts are found to contain Cu–O and Au–Au bonding only, with no Cu–Au interaction observed. The Cu–O bond lengths are in the range 1.92–1.97 Å which is typical for Cu(II)–oxygen interactions such as CuO²² (1.94 Å), copper oxalate²⁵ (1.98 Å) or Cu(II) nitrate²³ (1.96 Å, 1.99 Å). The Cu–O distance in Cu₂O is significantly shorter²⁶ (1.83 Å) and there is no evidence for it being present

Table 6 Catalyst test data: performance summary at 300 °C

Preparation method	Pretreatment	Propene conversion/%	Selectivity/%		
			Acrolein	Carbon dioxide	Oxygenates ^a
CuAu/SiO₂ catalysts					
Impregnation	Calcination	0.14	45	21	34
	Reduction in H ₂	0.28	41	36	23
	Reduction in H ₂ and calcination	0.20	83	17	0
	NaBH ₄ reduction	0.26	84	16	0
	NaBH ₄ reduction and calcination	0.20	82	18	0
Deposition	Reduction in H ₂	2.0	93	6	1
	Reduction in H ₂ and calcination	5.6	84	7	9
Cu/SiO₂ catalyst					
Impregnation	Calcination	0.22	85	15	0
Au/SiO₂ catalyst					
Impregnation	Calcination	0.09	74	26	0

^a Acetone, propene oxide and ethanal.

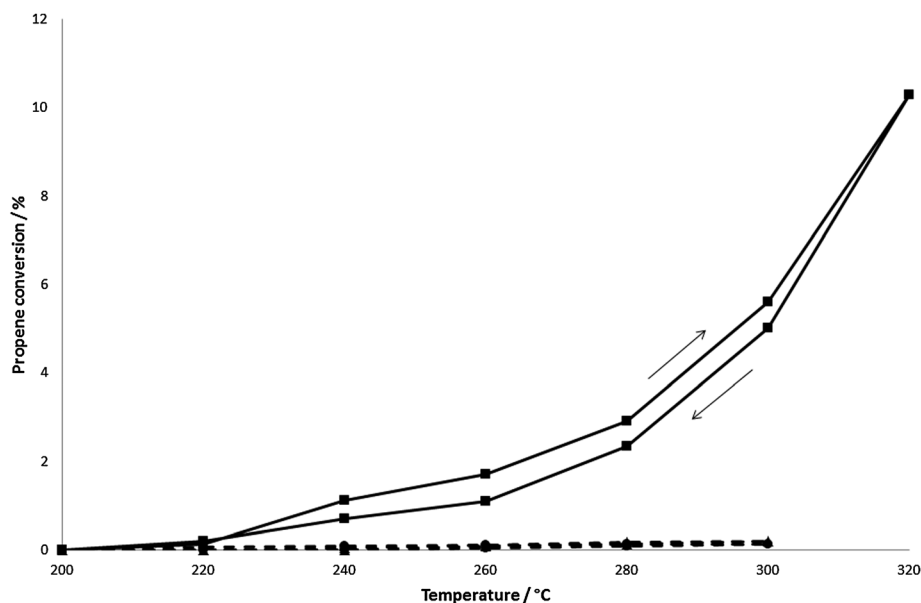


Fig. 7 Catalytic performance of CuAu/SiO₂ prepared by deposition followed by a reduction–calcination activation step. (solid line, square markers) Compared with catalysts prepared by impregnation (dashed lines) calcined only (circles) and reduced and calcined (triangles).

in these materials. The shortest Cu–O distances belong to the two hydrogen-reduced materials (1.92 and 1.93 Å) which could suggest a contribution from Cu₂O. However, the contribution would be very small as the bond distances are still close to that typical for CuO. The Au–Au distances are in the range 2.84–2.88 Å which are typical of gold metal²⁷ (2.86 Å). The two hydrogen-reduced samples contain a mixture of interatomic interactions: Cu–O, Cu–Au and Au–Au whilst the catalyst prepared by impregnation also has Cu–Cu co-ordination, in agreement with Meitzner *et al.*²¹ The Cu–Au distances calculated for the two hydrogen reduced materials are different (2.75 Å for the impregnated catalyst and 2.65 Å for the deposition catalyst) but both lie between the metal–metal distances for Cu–Cu²⁸ (2.56 Å) and Au–Au²⁷ (2.86 Å). The difference is likely to reflect differences in the composition of the alloys. Taking a Vegard's law approach to the bond distances²⁹ measured by EXAFS gives an

average composition of Au₆₃Cu₂₇ for the impregnated catalyst and Au₃₀Cu₇₀ for the deposition catalyst. XRD, for comparison, determined two CuAu phases in the impregnated catalyst: Au₉₃Cu₇ and Au₈₄Cu₁₆ whilst in the deposition catalyst the lattice parameter was the same as for monometallic gold catalysts (Table 3). The difference between XRD and EXAFS results suggests that for the impregnated catalyst, the most crystalline part of the sample (the largest particles) is gold rich whilst there are also copper-rich smaller nanoparticles. For the deposition sample, the CuAu phase is likely to be found in the smaller nanoparticles as it is not clearly observed by XRD.

Impact of preparation method

Changing the catalyst preparation method from impregnation to deposition has been shown to have a significant impact on

Table 7 Illustrative examples of copper and gold catalysts in propene oxidation

Catalyst	Reaction conditions	GHSV/l kg _{cat} ⁻¹ h ⁻¹	T/°C	Propene conversion/%	Major product (selectivity/%)	Ref.
0.06% CuO/SiO ₂	C ₃ H ₆ /O ₂ = 1/5	10.2	475	40	Acrolein (10)	32
0.67% Au/TiO ₂	C ₃ H ₆ /H ₂ /O ₂ = 1/1/1	4000	50	0.5	Propene oxide (95)	15
0.2% Au/TS-1	C ₃ H ₆ /H ₂ /O ₂ = 1/1/1	4000	200	0.6	Propanal (74)	15
1% Au/SiO ₂	C ₃ H ₆ /H ₂ /O ₂ = 1/1/1	4000	>200	<1	Acrolein, propanal, acetone, ethanal (NR)	33
1% Cu/SiO ₂ small particles	C ₃ H ₆ /O ₂ /He = 1/1/18	30 000	225	0.3	Propene oxide (50)	10
	C ₃ H ₆ /O ₂ /He = 1/1/18	30 000	360	3.3	Acrolein (35)	10
5% Cu/SiO ₂ larger particles	C ₃ H ₆ /O ₂ /He = 1/1/18	30 000	225	0.1	Acrolein (40)	10
	C ₃ H ₆ /O ₂ /He = 1/1/18	30 000	350	12.5	Acrolein (40)	10

NR = not reported.

catalyst performance. For example, considering the hydrogen-reduced and calcined catalysts, at 300 °C the rate of propene conversion is increased by a factor of almost thirty. A lot of this is likely to be a consequence of the smaller particle size of the catalysts prepared by deposition (around 5–10 nm) compared with those prepared by impregnation which can be much larger (upwards of 20 nm) and which TEM shows to contain larger metal clusters (Fig. 5) as well as small particles.

The other major impact of changing from an impregnation to a deposition method is to change the speciation of the metals on the catalyst. Comparing the hydrogen-reduced catalysts shows that synthesis by deposition gives rise to only a small amount of copper-gold alloy, whilst impregnation gives much more. However, given that the catalyst prepared by deposition is much more active, it can be assumed that the impact of the smaller particle size dominates any effect of the copper-gold alloy content.

Impact of reducing agent

Comparison of hydrogen reduction with chemical reduction is of interest as they are both industrially relevant and yet give quite different results. Hydrogen reduction is usually performed at elevated temperature (315 °C in this work) and is often used as it is 'clean', leaving no residues apart from water. Sodium borohydride reduction, in comparison, is a low temperature process although it is highly exothermic and difficult to control at larger scales. A washing step is also needed to remove the large amounts of boron and sodium which are present in NaBH₄.

In this study the two reduction methods gave quite different products. Hydrogen reduction leads to large particles of CuAu alloy and a material which was relatively poorly active. Sodium borohydride reduction led to smaller particles which were not alloyed and also some larger clusters, which appear to contain both copper and gold, on the surface of the catalyst particles (Fig. 5). These could be caused by the rapid evolution of gases (such as H₂ or NO_x) in the catalyst pores, ejecting solution and metal salts to the exterior of the particles (an effect which has been observed before³⁰).

Interestingly, the structure of the borohydride-reduced catalyst was very similar to the hydrogen-reduced and calcined material, giving a rapid, one-step synthesis of this material. In both cases EXAFS analysis determined the presence of copper oxide and gold metal on the catalyst. Their selectivity profiles are almost identical; however, the borohydride-reduced material was more active. This is reflected in the XRD pattern where

crystalline CuO is identified at 36° 2θ (Fig. 1A) in the hydrogen-reduced and calcined material, but is absent in the NaBH₄-reduced material. Of note is the gold peaks in the hydrogen-reduced and calcined sample which are very intense, making it the most crystalline gold of all the samples investigated. However, this is not detrimental to activity as the least active sample, the impregnated precursor reduced with sodium borohydride and calcined, has broader XRD lines than the equivalent material reduced using hydrogen, despite being only one-fifth as active. This shows that, as is often the case, not all the gold in the catalyst is relevant to catalysis.³¹

Comments on the nature of the active site

Probing the nature of the active site is a difficult task in heterogeneous catalysis due to the large number of different species present as we have shown in this catalyst system. In this case it is made more difficult since both copper and gold catalysts are active in propene oxidation. For copper catalysis, Cu/SiO₂ catalysts are known for the conversion of propene into acrolein. This reaction is usually run without the addition of hydrogen in the gas stream.³² We have previously reported the effect of hydrogen co-feeding in propene oxidation for CuAu/SiO₂ catalysts.³ The presence of Cu₂O on the catalyst is reported to be beneficial, whilst CuO is reported¹¹ to be responsible for complete combustion of propene to CO₂. Gold catalysts for propene oxidation are generally not supported on silica, with titania and titania-containing materials generally preferred. Gold-on-silica catalysts have been reported to be poorly active,³³ certainly when compared to equivalent materials on other, reducible, supports. Gold catalysts also tend to make propene oxide in propene oxidation with hydrogen co-feeding. Copper and gold catalysts tend to be used at different temperatures. The best results with gold catalysts are reported at low temperatures (<100 °C) whilst copper catalysts retain selectivity to acrolein even above 400 °C. The temperatures investigated in this study are therefore intermediate between the two. Illustrative examples of these catalysts are summarised in Table 7; this is not an exhaustive list.

Given the tendency for copper catalysts to make acrolein whilst gold catalysts make propene oxide on the oxidation of propene, it is reasonable to assume that the main active site in these catalysts is copper-based, since for the majority of materials the major product is acrolein. This prompts two

further questions – what is the nature of copper in the active site, and what is the role of the gold?

The fresh catalysts were characterised using EXAFS, which determined the presence of oxidic copper phases in many of the materials. The range of bond lengths determined is 1.93–1.97 Å, which shows the presence of a CuO-like phase. The Cu–O distance in Cu₂O is 1.83 Å²⁶ which is significantly shorter than the distance observed, which is more typical of CuO (1.94 Å²²). Also XANES fitting did not find a significant contribution of Cu₂O to any of the catalysts. The XANES spectrum of Cu₂O has a distinctive, sharp pre-edge which is not observed in any of the catalysts or precursors (Fig. 2A). Therefore the catalysts contain significant amounts of copper(II) oxide as the active phase. However, the performance of these catalysts is not the same as Cu/SiO₂ catalysts tested under the same regime – although performance at 300 °C is similar (Table 5), at lower temperatures the copper-only catalyst produces significant amounts of oxygenates (ESI†), which is not observed with the CuAu catalysts. This suggests that the presence of gold has an influence on the copper, but not by directly binding to it. This could be longer range interactions – such as those suggested by the TEM images of the borohydride-reduced and calcined catalyst prepared by impregnation (Fig. 5e). However, TEM images of other samples do not have the same conclusive evidence for this arrangement of copper and gold, and furthermore this is the least active sample of all those studied. Another possibility is that synthesis *via* an alloy leads to a well dispersed copper oxide phase. This is not interacting directly with the gold but instead it is dispersed onto the support. XRD shows that the copper oxide in these materials is well-dispersed, even the high temperature calcined materials only showing low intensity CuO reflections, when compared with the nearby gold metal reflection. Interestingly there is a sharp reflection at 36.2° 2θ in the most active catalyst, close to the main intensity reflection for CuO although slightly shifted to higher 2θ. The origin of this peak is not clear.

As we conclude that these catalysts do not contain Cu(I), this puts us at variance with the literature on copper-catalysed propene oxidation, where Cu(I) is generally proposed as an active species.¹¹ However, as described above we find no evidence for Cu(I) in any of our analyses. It is, of course, possible that Cu(I) is made during the reaction, by reduction of Cu(II) by either propene or hydrogen. Temperature-programmed reduction (TPR) analysis of a CuO/SiO₂ catalyst showed that the metal was reduced between 160–260 °C, with a very small fraction reduced at 260–340 °C (Fig. S7, ESI†). Hence reduction of copper(II) at reaction temperatures is feasible.

The exception to this discussion is the catalyst prepared by impregnation reduced with hydrogen which EXAFS shows to contain Cu–Au and Cu–Cu phases as well as gold metal and copper oxide. All of these phases are active catalysts in propene oxidation^{5,6,9} although the particle size is large, meaning that catalytic activity is low. The higher number of active sites contributes to the high selectivity to oxygenates (in this case, propene oxide), even at 300 °C.³

Good dispersion of the metal particles on the catalyst support (*i.e.* a small particle size) seems to be important in achieving good propene conversion: both of the most active catalysts have

small particles. However, comparison of the data in Tables 2 and 6 shows that there are other catalysts which contain small particles which are much less active. Clearly other factors, such as speciation, also have an impact. Also, for catalysts such as these which contain a range of metal species, measuring an accurate particle size is complicated by sample size and the laborious nature of particle counting (TEM) and the presence of large particles which do not participate in catalysis (XRD).

Effect of reaction temperature

We have studied the catalysts in propene oxidation in the temperature range 200–300 °C following a strict temperature protocol: the reaction was started at 200 °C and then increased in steps of 20 °C to 300 °C and then reduced in steps back to 220 °C. This allows us to understand changes in catalyst performance during catalysis (see ESI†). The stability of the catalysts varies greatly; some barely change whilst others change markedly over the temperature range. These changes are seen in both selectivity and activity. As steady-state data were recorded in each case, the changes must be caused by variations in the structure or performance of the active sites on the catalyst. Generally, the catalysts which had been reduced and calcined were the most stable over the temperature range, whilst the reduced-only materials tended to change more. The stability of the reduced-calcined catalyst might be expected; a catalyst which has been calcined at 675 °C could be expected to be stable at 300 °C. The reduced-only catalysts have not had this high temperature treatment and therefore might be expected to change more. Additionally, these materials have the greatest number of active sites³ and so the selectivity will change most with temperature. Indeed, the sodium borohydride-reduced catalyst displayed the greatest change with temperature. The nature of these changes is likely to be complex, and include effects such as sintering, carbon laydown, alloying or de-alloying. This is the subject of a further study.

Another general feature of the catalysts investigated is that selectivity to oxygenates tended to be observed at lower temperature (close to 200 °C), whilst at higher temperature (nearer 300 °C) acrolein and carbon dioxide were often the only two products observed. This is consistent with the expected behaviour of copper, gold and copper–gold catalysts (Table 7). At lower temperatures (≤200 °C), propene oxide is produced over all three systems.^{5,10,15} For gold catalysts, propanal is also produced.¹⁵ However, at higher temperatures (≥300 °C), acrolein is produced over copper¹⁰ and copper–gold⁵ catalysts. Our Au/SiO₂ catalyst, despite being poorly active, also made acrolein at temperatures above 260 °C (Table S1, ESI†). Making acrolein requires a different part of the propene molecule to be activated (CH₃ group) compared with making propene oxide (C–C double bond). It is possible, therefore, that a different adsorption geometry is required in each case.

Conclusions

This study has demonstrated that control of the properties of CuAu/SiO₂ catalysts through careful choice of synthesis method

and activation treatment can be used to tune their catalytic performance. Catalysts prepared by a two-step sequential deposition method showed greater activity than those prepared by impregnation, which is a consequence of their smaller particle size and therefore greater reactive surface area. The majority of the catalysts studied contain gold metal and well-dispersed copper oxide, and it is this latter phase which is thought to be the origin of the high selectivity to acrolein observed at higher temperature. The gold in the catalysts is only active at lower temperature and generally makes oxygenated products such as ethanal or acetone. The role of gold in the catalysts seems to be to mediate the synthesis of the well-dispersed copper oxide rather than to interact directly with the copper itself. Detailed catalytic studies showed that hysteresis is observed with some materials on cycling the temperature between 200 °C and 300 °C, and this is the subject of a further investigation.

Acknowledgements

The authors wish to thank Lubomira Duhackova, Godson Nnorom-Junior, James McNaught and Laura Stead for ICP analysis, Dr Kerry Simmance, Hoi Jobson, James McNaught and Dr Edward Bilbé for XRD analysis, Dr Jingshan Dong, Dr Gregory Goodlet and Dr Sarennah Longworth-Cook for TEM analysis and Dr Crina Corbos and Dr Jose Antonio Lopez Sanchez for help collecting the XAS data. CLB is grateful to Johnson Matthey for a PhD studentship. We acknowledge financial support from the European Union via the FP7 ELISA project for travel and sustenance for the collection of the XAS data.

References

- 1 C. L. Bracey, P. R. Ellis and G. J. Hutchings, *Chem. Soc. Rev.*, 2009, **38**, 2231–2243.
- 2 X. Liu, A. Wang, X. Wang, C.-Y. Mon and T. Zhang, *Chem. Commun.*, 2008, 487–489.
- 3 C. L. Bracey, A. F. Carley, J. K. Edwards, P. R. Ellis and G. J. Hutchings, *Catal. Sci. Technol.*, 2011, **1**, 76–85.
- 4 J. H. Sinfelt and A. E. Barnett, *U.S. Pat.*, 3989674, 1976.
- 5 R. J. Chimentão, F. Medina, J. L. G. Fierro, J. Llorca, J. E. Sueras, Y. Cesteros and P. Salagre, *J. Mol. Catal. A: Chem.*, 2007, **274**, 159–168.
- 6 J. Llorca, M. Dominguez, C. Ledesma, R. J. Chimentão, F. Medina, J. Sueiras, I. Angurell, M. Seco and O. Rossell, *J. Catal.*, 2008, **258**, 187–198.
- 7 C. D. Pina, E. Falletta and M. Rossi, *J. Catal.*, 2008, **260**, 384–386.
- 8 T. Pasini, M. Piccinini, M. Blosi, R. Bonelli, S. Albonetti, N. Dimitratos, J. A. Lopez-Sanchez, M. Sankar, Q. He, C. J. Kiely, G. J. Hutchings and F. Cavani, *Green Chem.*, 2011, **13**, 2091–2099.
- 9 T.-C. Ou, F.-W. Chang and L. S. Roselin, *J. Mol. Catal. A: Chem.*, 2008, **293**, 8–16.
- 10 O. P. H. Vaughan, G. Kyriakou, N. Macleod, M. Tikhov and R. M. Lambert, *J. Catal.*, 2005, **236**, 401–404.
- 11 J. B. Rietz and E. I. Solomon, *J. Am. Chem. Soc.*, 1998, **120**, 11487–11488.
- 12 N. Scotti, N. Ravasio, F. Zaccherra, R. Psaro and C. Evangelista, *Chem. Commun.*, 2013, **49**, 1957–1959.
- 13 P. M. Heyndrickx, J. W. Thybaut, H. Poelman, D. Poelman and G. B. Marin, *J. Catal.*, 2010, **272**, 109–120.
- 14 R. Zhang, D. Shi, Y. Zhao, B. Chen, J. Xue, X. Liang and Z. Lei, *Catal. Today*, 2011, **175**, 26–33.
- 15 B. S. Uphade, S. Tsubota, T. Hayashi and M. Haruta, *Chem. Lett.*, 1998, 1277–1278.
- 16 J. Chen, S. J. A. Halin, E. A. Pidko, M. W. G. M. Verhoeven, D. M. P. Ferrandez, E. J. M. Hensen, J. C. Schouten and T. A. Nijhuis, *ChemCatChem*, 2013, **5**, 467–478.
- 17 A. C. Gluhoi, N. Bogdanchikova and B. E. Nieuwenhuys, *Catal. Today*, 2006, **113**, 178–181.
- 18 E. Fonda, A. Rochet, M. Ribbens, L. Barthe, S. Belin and V. Briois, *J. Synchrotron Radiat.*, 2012, **19**, 417–424.
- 19 B. Ravel and M. Newville, *J. Synchrotron Radiat.*, 2005, **12**, 537–541.
- 20 T. Hayashi, K. Tanaka and M. Haruta, *J. Catal.*, 1998, **178**, 566–575.
- 21 G. Meitzner, G. H. Via, F. W. Lytle and J. H. Sinfelt, *J. Chem. Phys.*, 1985, **83**, 4793–4799.
- 22 H. Irie, K. Kamiya, T. Shibanuma, S. Mirura, D. A. Tryk, T. Yukoyama and K. Hashimoto, *J. Phys. Chem. C*, 2009, **113**, 10761–10766.
- 23 B. Morosin, *Acta Crystallogr.*, 1970, **B26**, 1203–1208.
- 24 H. Ruben, A. Zalkin, M. O. Faltens and D. H. Templeton, *Inorg. Chem.*, 1974, **13**, 1836–1839.
- 25 A. Micalowicz, J. J. Girerd and J. Goulon, *Inorg. Chem.*, 1979, **18**, 3004–3010.
- 26 J. Lee, T. Yano, S. Shibata, A. Nukui and M. Yamane, *J. Non-Cryst. Solids*, 2000, **277**, 155–161.
- 27 R. E. Benfield, D. Grandjean, M. Kröll, R. Pugin, T. Sawitowski and G. Schmid, *J. Phys. Chem.*, 2001, **105**, 1961–1970.
- 28 L. X. Chen, T. Rajh, Z. Wang and M. C. Thurnaner, *J. Phys. Chem. B*, 1997, **101**, 10688–10697.
- 29 S. N. Reifsnnyder and H. H. Lamb, *J. Phys. Chem. B*, 1999, **103**, 321–329.
- 30 P. R. Ellis, D. James, P. T. Bishop, J. L. Casci, C. M. Lok and G. J. Kelly, in *Advances in Fischer Tropsch Synthesis, Catalysts and Catalysis*, ed. B. H. Davis and M. L. Occelli, CRC Press, 2010, pp. 1–16.
- 31 Q. Fu, H. Saltsburg and M. Flytzani-Stephanopoulos, *Science*, 2003, **301**, 935–938.
- 32 H. Tüysüz, J. L. Galilea and F. Schüth, *Catal. Lett.*, 2009, **131**, 49–53.
- 33 T. A. Nijhuis, B. J. Huizinga, M. Makkee and J. A. Moulijn, *Ind. Eng. Chem. Res.*, 1999, **38**, 884–891.